Aerosol and Air Quality Research, 17: 2358–2366, 2017

ISSN: 1680-8584 print / 2071-1409 online
doi: 10.4209/aaqr.2017.01.0054

Application and Performance Test of a Small Aerosol Sensor for the Measurement of Aerosolized DNA Strands

Wenming Yang[1], Rong Zhu[2*], Chao Zhang[2], Zheng Li[3]

[1] *School of Mechanical Engineering, University of Science and Technology Beijing, Beijing 100083, China*
[2] *State Key Laboratory of Precision Measurement Technology and Instrument, Department of Precision Instrument, Tsinghua University, Beijing 100084, China*
[3] *Xi'an TianLong Science and Technology Co., Ltd., Xi'an 710018, China*

ABSTRACT

There is an immediate need for aerosol measuring sensors to monitor the size and concentration of DNA strand aerosols in PCR systems. We evaluate the performance of a previously developed small aerosol sensor for its potential use as a component in measuring DNA strand aerosols in PCR system chambers. A detailed derivation of the working principle is presented along with the principles used to determine the dimensions of the stages and the operational parameters. After characterizing the aerosolized DNA strands, experiments were conducted to identify their relationship with measured currents. The experimental results indicate that for aerosolized Escherichia coli DNA strands, the sensor is capable of measuring concentrations from 10^2 cm^{-3} to 10^5 cm^{-3} (from 10^3 cm^{-3} to 10^5 cm^{-3} for particles smaller than 102 nm) and sizes from 100 bp to 1000 bp. There was a slight difference between the results of the sensor and its theoretical model. The sensor exhibited good sensitivity to different concentrations and can detect every 150 bp of strands, indicating its effectiveness in monitoring ultrafine DNA strand aerosols for PCR systems and other applications.

Keywords: DNA strands; Small aerosol sensor; Aerosol measurement; PCR.

INTRODUCTION

Nowadays, polymerase chain reaction (PCR) based methods, in particular quantitative PCR are predominantly used as a molecular biological tool to replicate desoxyribonucleic acid (DNA), and can create copies of specific fragments of DNA by cycling through three temperature steps (Postollec *et al.*, 2011). Many systems based on quantitative PCR amplification of specific sequence have been developed (Chartier *et al.*, 2003; Le *et al.*, 2010). There are usually more than one reaction chambers in order to achieve high-throughput PCR amplification and to conduct many sequential PCR experiments simultaneously. During a PCR reaction, handling and processing sample fluid, and evaporation of samples may result in their invasion into the surrounding gas and subsequently forming DNA aerosol. It is possible for this aerosol to cause contamination and cross-talk of the PCR, and poses a risk of carry-over from experiments to experiments such that enlarges the possibility of failed amplification (Zhang *et al.*, 2006). Therefore, there is an immediate need of aerosol measuring devices to monitor the size and concentration of DNA strand aerosol in real time and to provide a warrant for decontamination and disinfection in chambers of PCR systems.

There are two general real-time ways to measure aerosol categorized according to their measurement principles. One is optical technique which detect aerosol by way of light, but most of the instruments based on this technique are not able to detect particles smaller than the wavelength of light that been used, namely, they lose sensitivity when they come to small particles (usually smaller than 100 nm (Kulkarni *et al.*, 2011)) and consequently cannot be used in the measurement of DNA strands. Condensation particle counters (CPC) are capable of detecting particles down to about 1 nm by condensation of supersaturated vapour onto particles and the following detection by light scattering (Winklmayr *et al.*, 1991).

Another method is based on electrical technique. Differential mobility analysis, combined with nanoelectrospray and online condensation particle counting, has been successfully applied in determining the mobility diameter of single-stranded and double-stranded DNA ranging from 6 kDa to 900 kDa (Mouradian *et al.*, 1997; Guha *et al.*, 2012). For this analytical technique, the nanoelectrospray converts a dilute analyte solution into a

* Corresponding author.
Tel.: +86-62788935; Fax: +86-62788935
E-mail address: zr_gloria@mail.tsinghua.edu.cn

series of droplets, which are then neutralized and converted into solvent-free nanoparticles. These nanoparticles are sized according to their gas-phase electrophoretic mobility in a differential mobility analyzer (DMA). As the voltage of the DMA is ramped, nanoparticles of increasing size sequentially exit the DMA and enter a CPC where they are counted. Coupling of nanoelectrospray and macro-ion mobility spectrometry with inductively coupled plasma mass spectrometer to determine the size of large biomolecules (proteins and DNA) was also demonstrated by Carazzone *et al.* (2008). Although these techniques have been used with satisfactory accuracy and precision (Laschober *et al.*, 2007), the involved instruments are large in size, expensive and complicated to use, which make them cannot be integrated into PCR systems.

Some examples of portable particle monitoring apparatuses combining differential mobility analysis and condensation particle counting technique were developed, such as WPS™ (Liu *et al.*, 2010), NanoScan (Tritscher *et al.*, 2013) and Kanomax PAMS 3300 (Hsiao *et al.*, 2016), whereas their sizes are still too large to be used in the limited space of PCR system chambers. There are also some aerosol sensors smaller in size purely based on diffusion charging and electrical detection, including NanoMonitor (Marra *et al.*, 2010), DiSCMini (Fierz *et al.*, 2011) and NanoCheck (Kulkarni *et al.*, 2011). In these sensors, aerosol is mixed with unipolar ions and then they attach to the aerosol particles by diffusion. Next, charges on the particles are measured using Faraday electrometer after removal of excess ions. These sensors can determine a number-weighted mean diameter and the number concentration of the particles in a diameter range from tens of nanometer to hundreds of nanometer. However, they have not been evaluated for the measurement of DNA strands.

In this study, tests of measuring aerosolized Escherichia coli DNA strands were carried out with a small aerosol sensor (SAS) to investigate its feasibility of monitoring the size and concentration of DNA strand aerosol in PCR systems. In our previous work (Yang and Zhu, 2014; Zhang *et al.*, 2016), a SAS was developed based on particle diffusion charging and inducted-current measurement, and its performance was tested for ultrafine NaCl aerosol particles. Fig. 1 schematically depicts the chip of the SAS. It consists of three stages (the charging stage, the precipitation stage and the sensing stage) made of pairs of printed circuit boards (PCBs). The two PCBs are bonded by a nonconductive film adhesive with fixed thickness h and there are copper layers connecting to ground to separate each stage and prevent the cross-talk among them.

However, dimensions of each stage and operation parameters of the SAS must be redetermined experimentally because of their different charging properties between DNA strands and NaCl particles. In this paper, a detailed derivation of the working principle was presented. Then principles of determining the dimensions of stages and the operation parameters were given for the purpose of meet the need of measuring aerosolized DNA strands. After characterization of the DNA particles, experiments were conducted to verify the applicability of the SAS in DNA aerosol measurement and to determine the relationships between measured currents and the size and concentration of DNA strands. Performance of this SAS employing the established relationships were tested by experiments of measuring reference DNA strands.

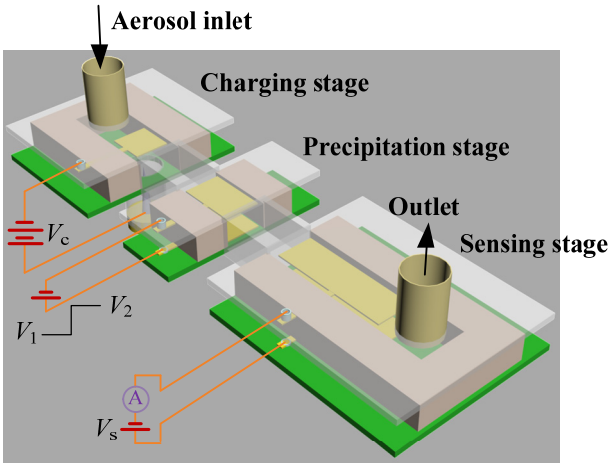

Fig. 1. Schematic of the sensor chip.

METHODS

Working Principle of the SAS

For the sensor chip shown in Fig. 1, a controlled aerosol flow ϕ is driven through the three stages successively by means of a pump situated at the outlet of the sensing stage. After entry the aerosol particles are electrically charged inside the charging stage via diffusion charging (Adachi *et al.*, 1985), which is enabled by a corona discharge formed between a tungsten needle-tip electrode mounted on one of the PCBs and a planar electrode on the opposite PCB. A sufficiently high positive voltage V_c generated by a high-voltage module is imposed on the needle-tip electrode to locally ionize the carrier gas. The produced positive ions drift from the discharge tip to the opposite electrode and a positive ion cloud is formed in the gap between the two electrodes. The aerosol particles become charged when they pass through the ion cloud region via diffusion charging.

After charging the particles enter into the precipitation stage and then the sensing stage, both of which are composed of two parallel planar electrodes plated on PCBs. The constant voltage V_s imposed on the sensing electrodes produces an electric field $E_s=V_s/h$ that is capable of precipitating substantially all the electrically-charged particles in the aerosol flow passing between the plates. One of the sensing plates is connected via an electrometer to a reference potential. Currents measured by the electrometer represent the precipitated amount of charges carried by the particles per unit time in the sensing stage. Since we need to obtain two characteristic parameters including particle number concentration N and average size $d_{p,av}$ of particles, two different inducted-current values are required during one measurement cycle. Thence, a biased block-shaped voltage pulse varying between $V_p = V_1$ and $V_p = V_2$ is applied to the electrodes of the precipitation stage. At the

low level ($V_p = V_1$), nearly all the charged particles traverse the precipitation stage unhindered but all the residual ions are removed because of their mobility disparities, while there are also a portion of charged particles captured inside the precipitation stage at the high level ($V_p = V_2$) due to the slightly higher electric field $E_p = V_2/h$. Accordingly, two different current values are acquired in the sensing stage ($I_s = I_1$ at $V_p = V_1$, $I_s = I_2$ at $V_p = V_2$, where $I_2 < I_1$).

When the low-level voltage is imposed on the precipitation stage, the number of particles in size d_p in the aerosol flowing through the sensor during time period Δt is $n_{d_p} = \varphi N(d_p)\Delta t$, where $N(d_p)$ is the size-distribution function of the aerosol, φ is the aerosol flow through the sensor. The quantity of charge carried by the particles in size d_p is $Q_{d_p} = \sum_{q=0}^{\infty} qe\varphi f_q(N_i t_r, d_p, q)N(d_p)\cdot\Delta t$, where q is the amount of elementary charges attracted on the particles, $e = 1.6 \times 10^{-19}$ C, f_q the fraction of particles in size d_p that are charged with q elementary charges. It is the function of d_p, q, and the product of ion density N_i and the residence time t_r. For an arbitrary distribution of aerosol, taking the example for that shown in Fig. 2, the total charge quantity on all the particles is

$$\Delta Q = \lim_{n\to\infty}\sum_{i=1}^{n}\sum_{q=0}^{\infty} qe\varphi f_q(N_i t_r, d_{pi}, q)N(d_{pi})\cdot\Delta t . \quad (1)$$

And the inducted current in the sensing stage will be

$$I_1 = \frac{\Delta Q}{\Delta t} = \lim_{n\to\infty}\sum_{i=1}^{n}\sum_{q=0}^{\infty} qe\varphi f_q(N_i t_r, d_{pi}, q)N(d_{pi}) . \quad (2)$$

Similarly, when the high-level voltage is imposed on the precipitation stage, the current is

$$I_2 = \lim_{n\to\infty}\sum_{i=1}^{n}\sum_{q=0}^{\infty} qe\varphi f_q(N_i t_r, d_{pi}, q)\cdot[1-\xi_q(d_{pi}, E_p)]N(d_{pi}) , \quad (3)$$

where $\xi_q(d_p, E_p)$ is the precipitated proportion of particles in size d_p charged with q elementary charges under the effect of electrical field E_p in the precipitation stage. At normal temperature and pressure, the Reynolds number of the flow in the sensor is $Re = 65000\ vh \le 130$ when $h \le 400$ μm and $v \le 5$ m s^{-1}, which indicates the flow is laminar. The slip flow regime specified by the Knudsen number $Kn = 0.1328 \times 10\ s^{-6}/d_p$ lying in the range from 0.885 to 13.2 for the aerosol particles in size ranging from 10 nm to 300 nm occurs in the aerosol system. Then $\xi_q(d_p, E_p)$ can be calculated according to the balance between drag force and electrostatic force for parallel plate structure of the precipitation stage as

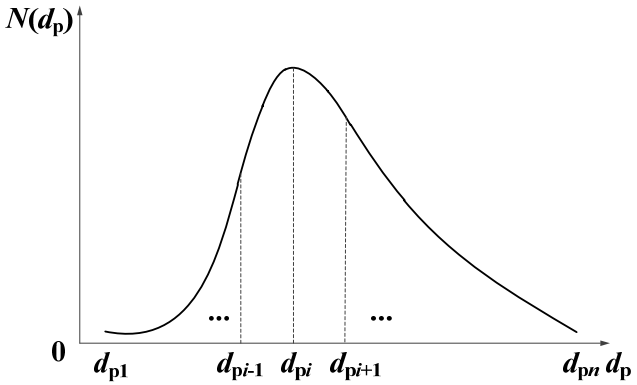

Fig. 2. One type of size distribution of aerosol.

$$\xi_q(d_p, E_p) = \frac{qeC_c E_p L_p}{3\pi\eta v d_p h} \quad (4)$$

on the non-mixing assumption, where L_p is the length of the electrode plates of the precipitation stage, η is the viscosity of carrier gas, v is the average air speed in the stage, C_c is the slip correction factor, which is nearly inversely proportional to d_p for spherical particles (Allen and Raabe, 1985), namely, $C_c(d_p) = C_1/d_p$ and C_1 is a constant.

The average number of elementary charges on a particle with diameter d_p can be expressed as

$$Q(d_p) = \sum_{q=0}^{\infty} q\cdot f_q(N_i t_r, d_p, q) . \quad (5)$$

As regards the direct charging stage of our sensor, the discharge current is about a few tenths of milliamperes by the action of an imposed voltage of nearly 1 kV. The order of magnitude of the estimated product $N_i\, t_r$ is 10^{13} m^{-3} s. Under such conditions, $Q(d_p)$ is roughly proportional to d_p for the range of 10 nm < d_p < 300 nm (Fuchs, 1963; Pui *et al.*, 1988; Kulkarni *et al.*, 2011), namely, $Q(d_p) = C_2 d_p$ and C_2 is a constant. Such that Eq. (2) can be simplified as

$$\begin{aligned} I_1 &= \lim_{n\to\infty}\sum_{i=1}^{n} e\varphi Q(d_{pi})N(d_{pi}) = C_2 e\varphi \lim_{n\to\infty}\sum_{i=1}^{n} d_{pi}N(d_{pi}) \\ &= C_2 e\varphi N d_{p,av} \end{aligned} \quad (6)$$

where $d_{p,av} = \lim_{n\to\infty}\sum_{i=1}^{n} d_{pi}N(d_{pi}) \Big/ N$.

According to Eq. (5), we can derive

$$Q(d_p)^2 = \left(\sum_{q=0}^{\infty} q\cdot f_q(N_i t_r, d_p, q)\right)^2 = \sum_{q=0}^{\infty} q^2\cdot f_q(N_i t_r, d_p, q) - \sum_{\substack{i=1,j=1 \\ i\neq j}}^{\infty} f_q^i(N_i t_r, d_p, q) f_q^j(N_i t_r, d_p, q)\left(q^i - q^j\right)^2 , \quad (7)$$

where $f_q < 1$ and q is usually less than 2 in the diameter range of 10–300 nm (Pui *et al.*, 1988). Thus the second term at the right side of Eq. (7) can be ignored and then we yield

$$\sum_{q=0}^{\infty} q^2 \cdot f_q(N_i t_r, d_p, q) \approx Q(d_p)^2 = C_2^2 d_p^2 . \quad (8)$$

Based on Eqs. (4) and (8) and the definition $N = \lim_{n\to\infty} \sum_{i=1}^{n} N(d_{pi})$, Eq. (3) can be simplified as

$$\begin{aligned} I_2 &= I_1 - \lim_{n\to\infty} \sum_{i=1}^{n} \sum_{q=1}^{\infty} qe\varphi f_q(N_i t_r, d_{pi}, q) \cdot \xi_q(d_{pi}, E_p) N(d_{pi}) \\ &= I_1 - \frac{e^2 \varphi E_p L_p}{3\pi\eta v h} \lim_{n\to\infty} \sum_{i=1}^{n} Q^2(d_{pi}) C_c N(d_{pi}) / d_{pi} \\ &= I_1 - \frac{C_1 C_2^2 e^2 \varphi E_p L_p}{3\pi\eta v h} N \end{aligned} \quad (9)$$

Combining Eq. (9) with Eq. (6), the following expressions of number-averaged size and number concentration for a definite sensor can be obtained.

$$d_{p,av} = S_{dp} \frac{I_1}{I_1 - I_2}, \quad (10)$$

$$N = S_N (I_1 - I_2), \quad (11)$$

where

$$S_N = \frac{3\pi\eta v h}{C_1 C_2^2 e^2 \varphi E_p L_p}, \quad (12)$$

$$S_{dp} = \frac{C_1 C_2 e E_p L_p}{3\pi\eta v h} . \quad (13)$$

They can be calibrated experimentally in specific applications. For instance, measurement of monodispersed particles with known size and concentration could establish the relationships between the size and concentration with the corresponding I_1 and I_2. Accordingly, the values of coefficients S_N and S_{dp} could be obtained.

Determination of the Dimensions and Operation Parameters of the Sensor Chip

Dimensions of each stage and operation parameters of the sensor can be determined according to electrostatic principle and some experimental results. It is also a tradeoff between normal operation of corona discharge and measurement of weak current signals. This is because it is better to reduce the flow rate to gain a higher charging efficiency and a less disturbance to the discharge. However, the electrometer prefers larger flow volume in order to relieve the requirement of higher measurement accuracy.

The three stages are integrated into a whole minimized sensing ship and the flow channels inside are identical in width and height for ease of manufacturing. The height of the channel h is determined by the compromise between the corona inception voltage and the leakage current in the sensing stage and the width w is educed from the experimental results of ion drift scope of corona discharge. The velocity of the aerosol flow v is the maximum one that will not disturb the discharge severely.

The low-level voltage V_1 applied on the precipitation stage and the length of its electrode plate L_p should satisfy the relationship $V_1 L_p = h^2 v / eB_{air}$ for the sake of removing all the residual ions, where B_{air} is the mobility of air molecular. The value of V_1 was verified experimentally by gradually increasing of it when only pure air was driven through the sensor until the current observed in the sensing stage was the same as that when there was not any air flow. However, there must not be too much loss of the smallest particles been measured due to this electric field. The loss ratio caused by the electric field can be estimated as $\eta = neV_2 B_{d_p} L_p / (h^2 v)$, where B_{d_p} is the particle mobility. According to this estimation, the loss ratio of particles with diameter of 20 nm is less than 0.6% in an actual design if the diffusion loss was neglected. Theoretically, the loss ratio of particles larger than 20 nm should be much smaller than this estimated value. The selection of high-level voltage V_2 should be ensured that the smallest particles must not be completely removed and meanwhile, the largest ones should be partly precipitated. Moreover, there must be a sufficient difference between V_1 and V_2 to guarantee a proper discrimination of I_1 with I_2 by the electrometer.

The length of the sensing electrodes L_s in the sensing stage relates to the applied voltage V_s by $L_s \geq h^2 v / (eV_s B_m)$ so as to collect all the charged particles. B_m is the mobility of the largest particles to be measured. And V_s must not be too high to avoid gas ionization between the electrodes. For one type of design, V_s was set to 5 V when L_s = 40 mm.

The completed sensor is shown in Fig. 3, in which only the sensor chip is assembled inside the instrument while other components could be connected with the chip through pipelines and wires from the inside out in practical applications. The size of the whole device is about 12 × 12 × 5 cm and that of its main components are given in Table 1.

Characterization of DNA Aerosol Particles

In our study, Escherichia coli DNA particles were

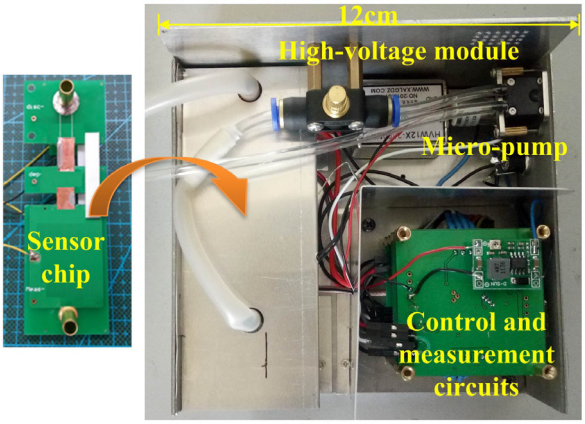

Fig. 3. The photo of the aerosol sensor.

Table 1. Sizes of the main components of the sensor (units: cm).

Sensor chip		Micro-pump		High-voltage modular		PCB of Circuits	
Length	Width	Length	Width	Length	Width	Length	Width
10	2	3	1.5	2.7	1.5	4.2	4.2

generated by aerosolization of DNA solutions suspended with monodisperse DNA strands, which were made from separation and purification of DNA markers (DL 1000 and DL 5000, Takara Bio Inc.) using HPLC method. To examine the size of the aerosolized DNA strands, they were collected on filter papers and then tested by SEM. Fig. 4 shows one of the SEM images of the DNA particles collected by air filter, the effective size of which is characterized as their strand length. It is consistent with the relationship $d_p \approx 0.34 \cdot N_t$ (Robert, 2011), where N_t is the number of base pairs (bp) composing the strands. We can also find from SEM experiments that the strands were less likely to curl themselves when $N_t < 1500$ bp. Thence the effective size of the aerosolized DNA strands could be obtained by N_t using above transform formula.

The aerosol generator (ATM-220, TOPAS) used to aerosolize the DNA solutions with different concentration of suspended DNA strands was calibrated employing a CPC (3776, TSI) to obtain the number concentration of that dispersed in aerosol. During the experiments, inlet pressure and concentration of DNA solution were adjusted to obtain DNA aerosol with specific number concentration.

Experiment Setup

Using different DNA markers (from DL 1000–100 to 1000–1000 corresponding to effective size of DNA particles from 34 nm to 340 nm) and strand solutions with different number concentration, DNA aerosol samples with particle number concentration of 10^2–10^5 cm^{-3} were generated by aerosolization. The experimental setup shown in Fig. 5 allows aerosolization of DNA strands from their liquid suspensions and the DNA aerosol detection by the sensor, in which all the circuits and the micropump are integrated with the sensor given in Fig. 3. The oscilloscope is used to monitor the stability of corona discharge. Three repeated measurements were conducted under each condition for evaluating statistics.

RESULTS AND DISCUSSION

Fig. 6 shows the relationship between the number concentration N of DNA strands and the measured $I_1 - I_2$ in the cases of different strand sizes. $I_1 - I_2$ increases linearly with the number concentration, which is similar to that predicted by Eq. (11). However, there are intercepts with the horizontal abscissa. Linear fits were conducted and the relationship could be expressed as

$$N = 83326 \times (I_1 - I_2) - 204162, \quad (14)$$

where the units are cm^{-3} (for N) and pA (for I_1 and I_2), respectively. $St(N)$ in Fig. 6(a) is the standard deviation of $(I_1 - I_2)$ values of particles with different sizes for certain number concentration N. The $St(N)$ value is relatively larger for higher concentrations, but all of them are smaller than 0.05. Therefore, the number concentration is supposed to

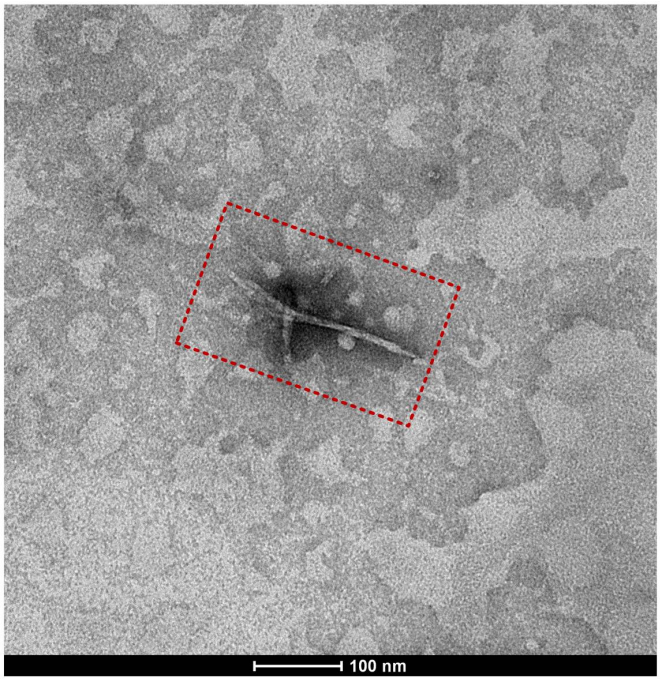

Fig. 4. SEM image of one DNA strand (DL 1000–500).

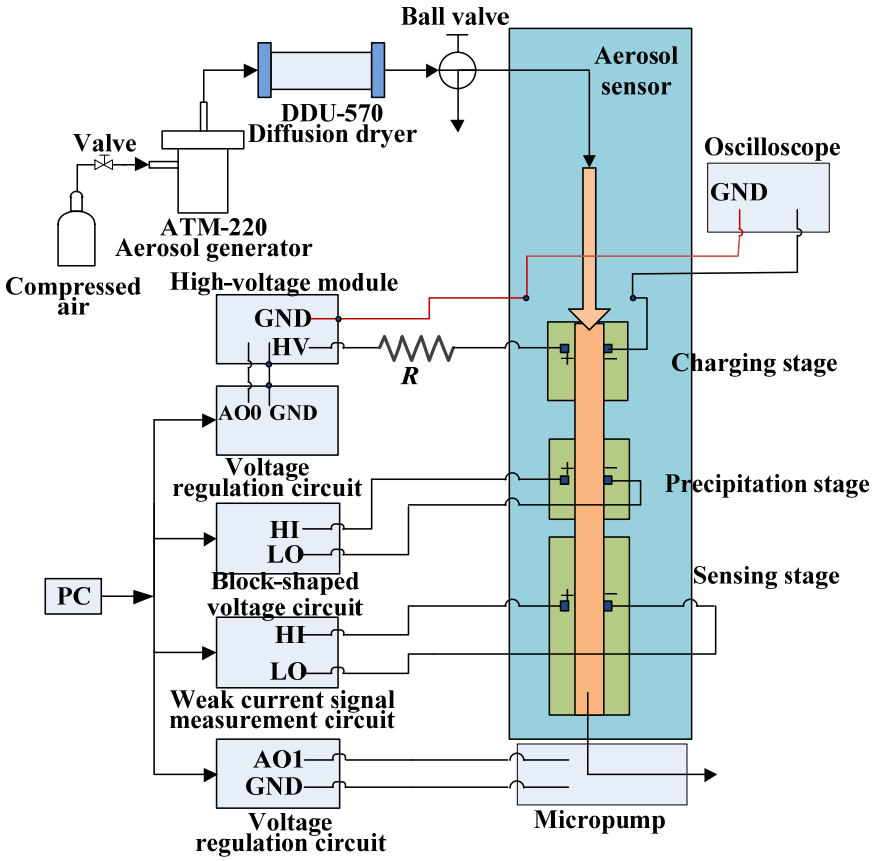

Fig. 5. Schematic of experimental set-up.

be independent of size in this research. In most cases, the sensor could measure the number concentration of DNA strands ranging from 10^2 cm^{-3} to 10^5 cm^{-3}, but it failed when the size was less than 102 nm. In our experiments, the lowest measurable concentration of the sensor was 10^3 cm^{-3} for particles in the size range of 34–102 nm. It is because the smaller the particles are, the less possibility for them to be charged, such that the induced current is too weak to be sensed by the electrometer (which has a resolution of 50 fA) in the sensing stage.

As for the particle size detection, there are also linear relationships between $I_1/(I_1 - I_2)$ and the size of DNA strands in the range of 34–340 nm. However, the slopes and offsets of these relationships vary with number concentration, as is evident in Fig. 7. They can be summarized as

$$d_p = K(N) \times \frac{I_1}{I_1 - I_2} - b(N), \quad (15)$$

where $K(N)$ and $b(N)$ represent slope and offset as a function of N, respectively, which can be expressed as

$$K(N) = 2081 - 268 \times \log N, \quad (16)$$

$$B(N) = 1788 - 139 \times \log N. \quad (17)$$

Fitting of the results in the cases of different number concentration is shown in Fig. 8.

The difference between the experimental results and the theoretical model is supposedly attributed to the slip correction factor C_c, which was considered to be reversely proportional to d_p. It is true for sphere particles, but may not be suitable for DNA strands since the charging level depends on shape of particles (Oh *et al.*, 2004). Another reason may be that not all residual ions were removed during the low level voltage applied on the precipitation stage. This level cannot be set too high to bring about too much loss of charged particles to be measured.

Based on the above mentioned analysis, the aerosol sensor can figure out the number concentration of aerosolized DNA strands from the relationship between N and $I_1 - I_2$ given by Eq. (14). And then derives the size from the relationships between d_p and $I_1/(I_1 - I_2)$ described by Eqs (15)–(17). Comparison between the measured results and the reference data is shown in Figs. 9 and 10. Note that the sensor exhibits a good detectability to different number concentration in the range of 10^2–10^5 cm^{-3} (10^3–10^5 cm^{-3} for particles in size less than 102 nm), but the measurement error becomes larger for the lower concentration of 10^2 cm^{-3}, that is with a relative error of 33.3%. As for the size, the sensor is capable of detecting every 50 nm (corresponding to 150 bp) of the strands with a relative error of 64%–6.9%. One source of error may come from the random distribution of ions on the chains before they enter into the sensor.

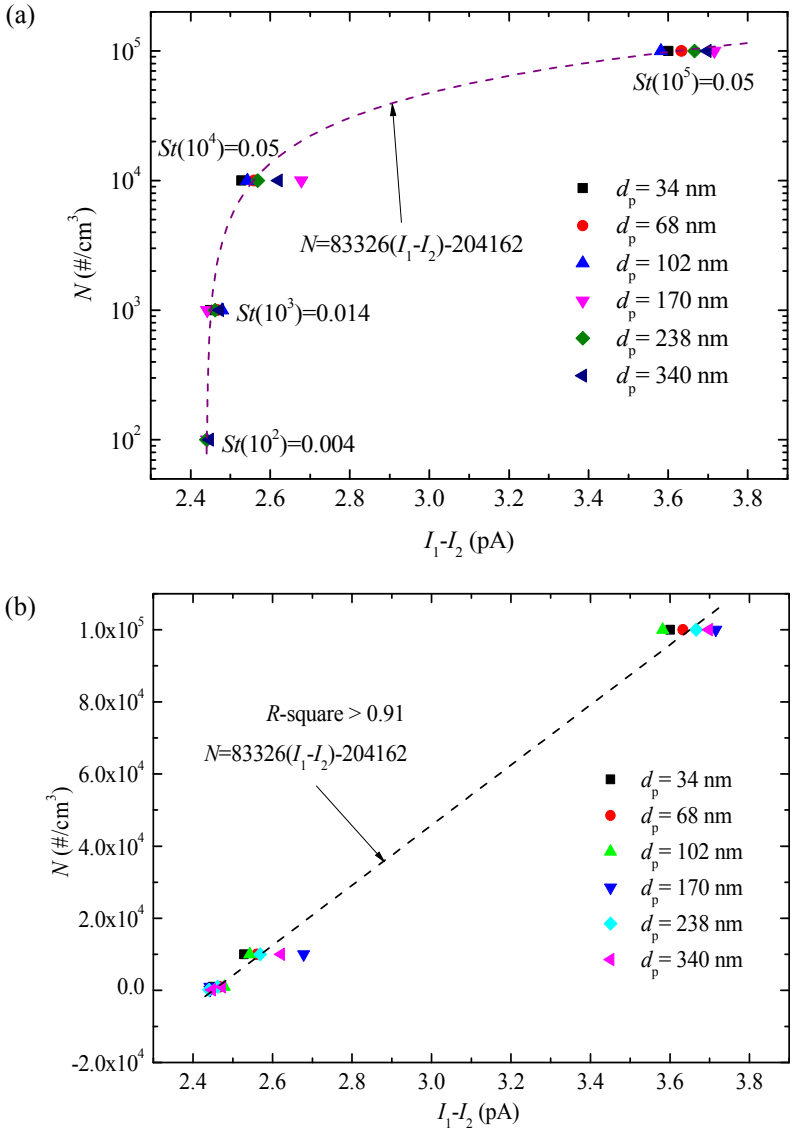

Fig. 6. Number concentration N of DNA strands as a function of $I_1 - I_2$ for different strand sizes. (a) figure with logarithmic scales; (b) figure with linear scales.

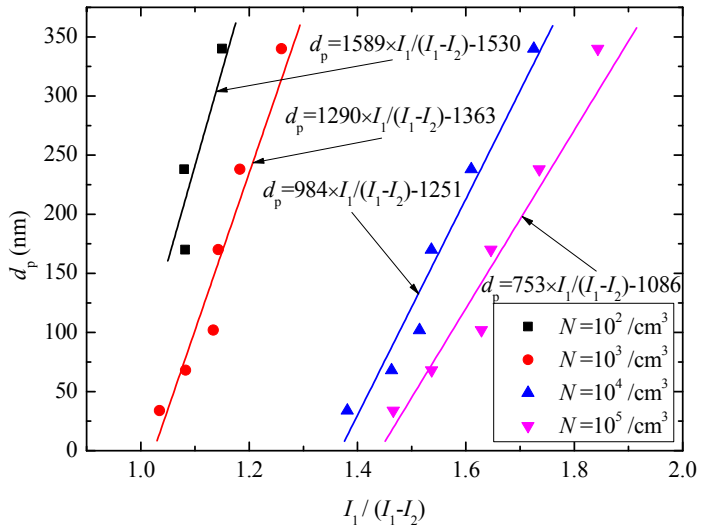

Fig. 7. Size of DNA strands as a function of $I_1/(I_1 - I_2)$ for different strand number concentration.

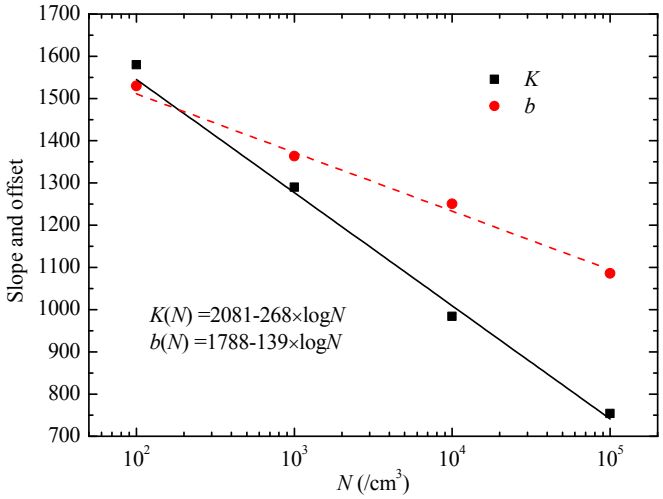

Fig. 8. Slope and offset corresponding to different number concentration.

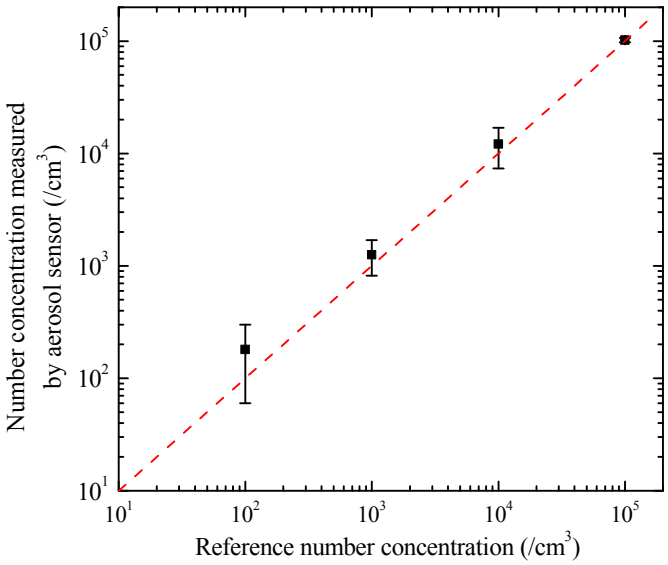

Fig. 9. The comparison between the measured results of number concentration by the aerosol sensor and the reference data.

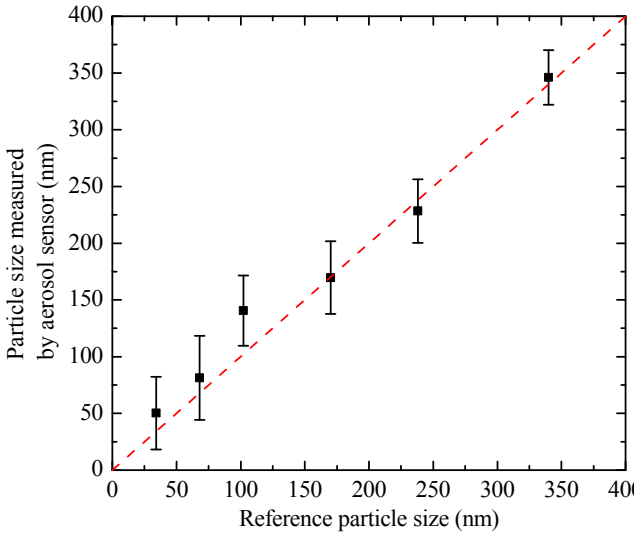

Fig. 10. The comparison between the measured results of size by the aerosol sensor and the reference data.

CONCLUSIONS

A previously developed small aerosol sensor based on diffusion charging and electrical detection was used to detect DNA strand aerosols in real time. The sensor is capable of measuring concentrations ranging from 10^2–10^5 cm^{-3} (10^3–10^5 cm^{-3} for particles smaller than 102 nm) and sizes ranging from 34–340 nm (corresponding to 100–1000 bp) for aerosolized Escherichia coli DNA strands. The sensor accurately detects different concentrations and sizes of DNA strands, demonstrating its ability to monitor ultrafine DNA strand aerosols. Our future research aims to improve the performance of the sensor, including measurement accuracy.

ACKNOWLEDGMENTS

This work was supported in part by the National Key Project of Scientific Instrument and Equipment Development under Grant 2012YQ03026, and the Fundamental Research Funds for the Central Universities under Grant FRF-TP-15-028A1.

REFERENCES

Adachi, M., Kousaka, Y. and Okuyama, K. (1985). Unipolar and bipolar diffusion charging of ultrafine aerosol particles. *J. Aerosol Sci.* 16: 109–123.

Allen, M.D. and Raabe, O.G. (1985). Slip correction measurements of spherical solid aerosol particles in an improved Millikan apparatus. *Aerosol Sci. Technol*. 4: 269–286.

Carazzone, C., Raml, R. and Pergantis, S.A. (2008). Nanoelectrospray ion mobility spectrometry online with inductively coupled plasma-mass spectrometry for sizing large proteins, DNA, and nanoparticles. *Anal. Chem*. 80: 5812–5818.

Chartier, I., Sudor, J., Fouillet, Y., Sarrut, N., Bory, C. and Gruss, A. (2003). Fabrication of an hybrid plastic-silicon microfluidic device for high-throughput genotyping. *Proc. SPIE* 4982: 208–219.

Fierz, M., Houle, C., Steigmeier, P. and Burtscher, H. (2011). Design, calibration, and field performance of a miniature diffusion size classifier. *Aerosol Sci. Technol*. 45: 1–10.

Fuchs, N.A. (1963). On the stationary charge distribution on aerosol particles in a bipolar ionic atmosphere. *Geofis. Pura Appl.* 56: 185–193.

Guha, S., Li, M., Michael, J.T. and Michael, R.Z. (2012). Electrospray–differential mobility analysis of bionanoparticles. *Trends Biotechnol*. 30: 291–300.

Hsiao, T.C., Lee, Y.C., Chen, K.C., Ye, W.C., Sopajaree, K. and Tsai, Y.I. (2016). Experimental comparison of two portable and real-time size distribution analyzers for nano/submicron aerosol measurements. *Aerosol Air Qual. Res*. 16: 919–929.

Kulkarni, P., Baron, P.A. and Willeke, K. (2011). *Aerosol measurement, principles, techniques, and applications*, 3rd ed., Wiley, New Jersey.

Laschober, C., Kaddis, C.S., Reischl, G.P., Loo, J.A., Allmaier, G. and Szymanski, W.W. (2007). Comparison of various nano-differential mobility analyzers (nDMAs) applying globular proteins. *J. Exp. Nanosci*. 2: 291–301.

Le, D.G., Mounier, J., Vasseur, V., Arzur, D., Habrylo, O. and Barbier, G. (2010). Quantification of Penicillium camemberti and Proqueforti mycelium by realtime PCR to assess their growth dynamics during ripening cheese. *Int. J. Food Microbiol*. 138: 100–107.

Liu, B.Y.H., Romay, F.J., Dick, W.D., Woo, K.S. and Chiruta, M.A. (2010). Wide-range particle spectrometer for aerosol measurement from 0.010 μm to 10 μm. *Aerosol Air Qual. Res.* 10: 125–139.

Marra, J., Voetz, M. and Kiesling, H.J. (2010). Monitor for detecting and assessing exposure to airborne nanoparticles. *J. Nanopart. Res.* 12: 21–37.

Mouradian, S., Skogen, J.W., Dorman, F.D., Zarrin, F., Kaufman, S.L. and Smith, L.M. (1997). DNA analysis using an electrospray scanning mobility particle sizer. *Anal. Chem*. 69: 919–925.

Oh, H., Park, H. and Sangsoo, K. (2004). Effects of particle shape on the unipolar diffusion charging of nonspherical particles. *Aerosol Sci. Technol*. 38: 1045–1053.

Postollec, F., Falentin, H., Pavan, S., Combrisson, J. and Sohier, D. (2011). Recent advances in quantitative PCR (qPCR) applications in food microbiology. *Food Microbiol*. 28: 848–861.

Pui, D.Y.H., Fruin, S. and McMurry, P.H. (1988). Unipolar diffusion charging of ultrafine aerosols. *Aerosol Sci. Technol*. 8: 173–187.

Robert, F.W. (2011). *Molecular biology*, 5th ed., McGraw-Hill, New York.

Tritscher, T., Beeston, M., Zerrath, A.F., Elzey, S., Krinke, T.J., Filimundi, E. and Bischof, O.F. (2013). NanoScan SMPS–A novel, portable nanoparticle sizing and counting instrument. *J. Phys. Conf. Ser.* 429: 012061

Winklmayr, W., Reischl, G.P., Lindner, A.O. and Berner, A. (1991). A new electromobility spectrometer for the measurement of aerosol size distributions in the size range from 1 nm to 1000 nm. *J. Aerosol Sci*. 22: 289–296.

Yang, W. and Zhu, R. (2014). In *A PCB type aerosol sensor for measuring nanoscale aerosol particles*. Kallio, P. (Ed.), 4th Int. Conference 3M. Nano. Taipei, Taiwan, 2014, IEEE, USA, pp. 85–89.

Zhang, C., Xu, J., Ma, W. and Zheng, W. (2006). PCR microfluidic devices for DNA amplification. *Biotechnol. Adv*. 24: 243–284.

Zhang, C., Zhu, R. and Yang, W. (2016). A micro aerosol sensor for the measurement of airborne ultrafine particles. *Sensors* 16: 399.

Received for review, January 25, 2017
Revised, August 16, 2017
Accepted, August 25, 2017